# A three-dimensional underwater sound propagation model for offshore wind farm noise prediction

Ying-Tsong Lin, Arthur E. Newhall, James H. Miller, Gopu R. Potty, and Kathleen J. Vigness-Raposa

Citation: The Journal of the Acoustical Society of America **145**, EL335 (2019); doi: 10.1121/1.5099560

View online: https://doi.org/10.1121/1.5099560

View Table of Contents: https://asa.scitation.org/toc/jas/145/5

Published by the Acoustical Society of America

# A three-dimensional underwater sound propagation model for offshore wind farm noise prediction

**Ying-Tsong Lin**[a] **and Arthur E. Newhall**
*Woods Hole Oceanographic Institution, Woods Hole, Massachusetts 02543, USA*
*ytlin@whoi.edu, anewhall@whoi.edu*

**James H. Miller and Gopu R. Potty**
*University of Rhode Island, Narragansett, Rhode Island 02881, USA*
*miller@uri.edu, gpotty@uri.edu*

**Kathleen J. Vigness-Raposa**
*Marine Acoustics, Inc., Middletown, Rhode Island 02841, USA*
*kathleen.vigness@marineacoustics.com*

**Abstract:** A three-dimensional underwater sound propagation model with realistic ocean environmental conditions has been created for assessing the impacts of noise from offshore wind farm construction and operation. This model utilizes an existing accurate numerical solution scheme to solve the three-dimensional Helmholtz wave equation, and it is compared and validated with acoustic transmission data between 750 and 1250 Hz collected during the development of the Block Island Wind Farm (BIWF), Rhode Island. The variability of underwater sound propagation conditions has been investigated in the BIWF area on a temporal scale of months and a spatial scale of kilometers. This study suggests that future offshore wind farm developments can exploit the seasonal variability of underwater sound propagation for mitigating noise impact by scheduling wind farm construction during periods of high acoustic transmission loss. Discussions on other applications of soundscape prediction, planning, and management are provided.

**Date Received:** February 20, 2019 **Date Accepted:** April 10, 2019

## 1. Introduction

The Block Island Wind Farm (BIWF), located 3.8 miles southeast of Block Island, Rhode Island, is the first U.S. commercial offshore wind farm[1] constructed for harvesting wind energy to generate electricity using five 6-MW General Electric wind turbines. *In situ* underwater and airborne sound measurements were made during the pile driving of the turbine jacket foundation installations and also during part of the first 2-year operational period.[2] A three-dimensional (3D) underwater sound propagation model has been created using a high-resolution bathymetric database and a data-assimilated ocean dynamic model for noise propagation prediction beyond the coverage of the *in situ* listening measurements. The research objectives of this modeling effort include (1) investigation of efficient and effective approaches to integrate acoustics and ocean circulation simulation tools and environmental databases, (2) understanding, predicting, and exploiting temporal and spatial variability of underwater sound propagation for mitigating wind farm construction noise impacts, and (3) ultimately, to establish an underwater soundscape modeling, predicting, and planning software system for noise impact management at future offshore wind farm sites.

Validation of the present sound propagation model with a set of broadband transmission data between 750 and 1250 Hz collected in the BIWF area was performed and is documented in this paper. The goodness of fit of the model predictions to the data was sufficient for making confident predictions on underwater noise propagation in the field. Specifically, the model was used to study pile driving noise propagation in two different seasons to contrast the Sound Exposure Level (SEL) of the noise and its kurtosis (the fourth standardized moment), which is an indication of the impulsiveness of a signal. The variance of a high kurtosis signal is the result of infrequent, extreme

[a]Author to whom correspondence should be addressed.

deviations as opposed to frequent, modestly sized deviations. Because of the high peak pressures associated with impulsive signals, kurtosis can characterize the potential impacts to marine mammals from such signals.[3] The seasonal variability on noise propagation originating from the BIWF turbines will be detailed in this paper.

This manuscript is organized as follows. First, a summary of water column variability that affects sound propagation is provided in Sec. 2. Then, descriptions and validation of the 3D underwater sound propagation model at the BIWF are provided in Sec. 3. The temporal and spatial dependence of acoustic propagation is covered in Sec. 4. The paper is concluded in Sec. 5 with summaries and future research plans.

## 2. Seasonal water column variability at the BIWF site

Variability of water temperature and salinity in the ocean produces changes in sound speed and consequently affects undersea acoustic propagation. This environmental variability spans broad time scales from minutes to seasons. In the BIWF area, the seasonal variability is notable in altering the general sound propagation pattern, which is discussed in this section.

In the summer, the water column is characterized by a strong thermocline[4] with up to an 8 °C decline in less than 10 m in the middle of the water column (20 m). This thermocline can produce a significant negative sound speed gradient of $-3.2\,s^{-1}$ and generates a downward refracting propagation condition. This negative sound speed gradient causes acoustic rays to bend toward the seafloor and interact with the bottom at large angles creating a higher bottom reflection loss.

In other seasons, the surface water cools due to less solar heat and atmosphere conditions, so the thermocline weakens. In addition, strong winds and storms (especially during the winter season) enhance water column mixing. Hence, the water temperature becomes colder compared to the summer and can be nearly constant from the sea surface to the sea floor. This can produce a constant sound speed (isovelocity) condition and more omni-directional propagation, in contrast to downward refracting propagation seen in the summer, so less bottom reflection loss from smaller incident angles is expected. Besides, colder water temperatures can cause a lower sound speed, which increases the acoustic impedance difference at the water-bottom interface (the sea floor) and the total reflection angle from the seabed as compared to summer. As a result, the lower-temperature and isovelocity water column sound speed profile will enhance long distance propagation of underwater sound.

## 3. Model description and validation

To understand, predict, and exploit temporal (hourly, daily, monthly, and seasonal) and spatial (on-site, local, and regional) variability of underwater sound propagation, a 3D propagation model has been created that incorporates realistic bathymetry, oceanography, and geology for environmental input. This model utilizes the parabolic-equation approximation, which has long been recognized as one of the most efficient and effective numerical methods to predict sound propagation in complex environments.[5] The advantage of this method is that it converts the two-way Helmholtz wave equation of elliptic type to a one-way wave equation of parabolic type, which enables efficient marching solution algorithms to reduce the computational resources for modeling 3D sound propagation.

The bathymetric input to the 3D propagation model, shown in Fig. 1(a), was from the 3 arc sec U.S. Coastal Relief Model[6] (CRM) that has a 100-m horizontal resolution. The water temperature and salinity were extracted from the Regional Ocean Modeling System (ROMS) ESPreSSO (Experimental System for Predicting Shelf and Slope Optics) model[7] covering the Mid-Atlantic Bight, as shown in Fig. 1(b), with a 5 km horizontal resolution, 36 terrain-following vertical levels, and a 1 h output interval. The ROMS ESPreSSO model is a data-assimilated model, and it captures spatial and temporal variations of physical oceanographic conditions. This improves the prediction of the acoustical variability due to time-varying ocean variations. However, it does not have the resolution to include kilometer scale oceanographic effects, such as internal waves. To include these small-scale effects is beyond the scope of this paper and hence proposed for future research. The geoacoustic properties of the seabed in the model were given to be sound speed 1725 m/s, density 1.8 g/cm$^3$, and attenuation coefficient 0.5 dB/$\lambda$, characterizing the sandy sediments in the BIWF area based on the Deck41 seafloor surficial sediment database.[8]

A broadband acoustic transmission experiment was conducted during the deployment cruise of the BIWF operation monitoring hydrophone arrays on December 21, 2016. The purpose was to collect a set of acoustic transmission data for validating the sound propagation model. The broadband signals (750–1250 Hz chirps)

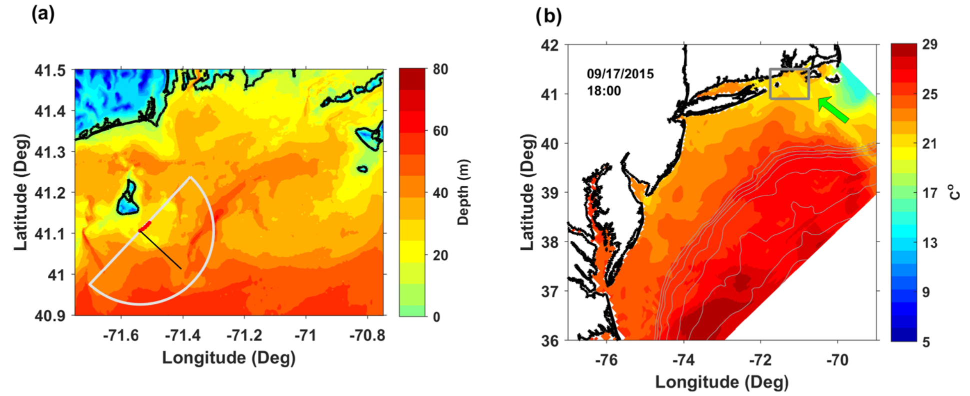


Fig. 1. (Color online) (a) Bathymetry at the BIWF location from the 3 arc sec U.S. CRM. Also included are the 3D sound propagation model domain in a semi-circle and a line showing the propagation modeling track shown in the paper. The red curve indicates the aperture of the wind turbine array. (b) Surface temperature from the ROMS ESPreSSO model is shown for September 17, 2015, during the BIWF development period.

were transmitted from a source towed at a depth of 5.5 m by the R/V Tioga (the work vessel for the mooring deployment operated by the Woods Hole Oceanographic Institution) along the solid track shown in Fig. 1(a) and received by a fixed vertical hydrophone array located at the end of the track in deeper water. A time series of the received signals at a depth of 32.7 m after pulse compression is plotted in the left panel of Fig. 2 as a stacked diagram with the vertical axis representing the source-to-receiver (S2R) distance in kilometers. The horizontal axis of the signal stacked diagram is the reduced arrival time calculated by subtracting the nominal travel time S2R/1.485 s (where 1.485 km/s is the average sound speed in the water column) from the actual travel time. This is to align the received signals, so one can better observe the change of the received pulses as a function of S2R.

3D and two-dimensional (2D) broadband propagation model outputs are shown in Fig. 2. Both of the model outputs are in general agreement with the data, and the model differences are small but notable in the later arrivals of higher propagation angles. This indicates that the specific propagation track along which the validation data were collected does not have the environment to support out-of-plane (3D) propagation. However, it will be shown in the next example for complete spatial variability in the BIWF area that 3D effects can be important along other propagation paths. Further discussions of data-model comparisons along the validation track are provided below. The model as it captures the time where the pulse terminates at closer S2R ranges less than 3000 m, shows that the model produces a total reflection angle at the bottom agreeing with the real value. Besides, the modeled arrival time agrees well with the data with a small error rate of 1 msec/km. The model also produces the observed multipath structure and intensity decay as a function of the S2R distance. One data feature that the model does not capture is the attenuation of later arrivals at long ranges. This is because the model does not take into account the spatial variation of bottom acoustic properties, which need more resources to completely collect. In

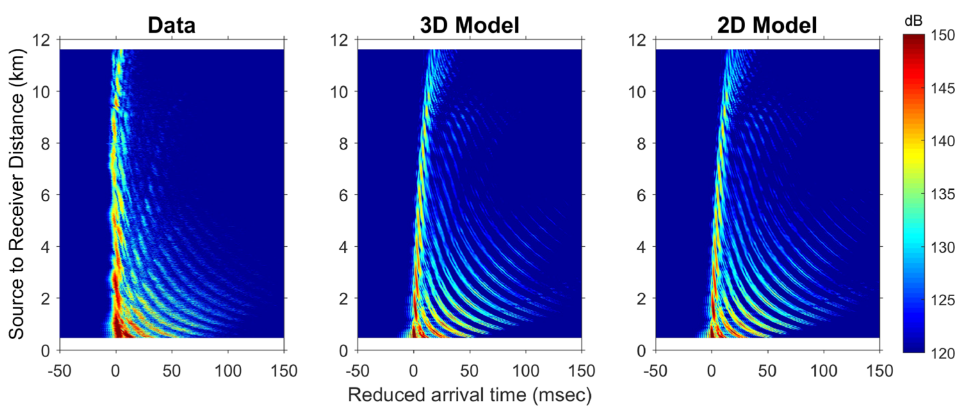


Fig. 2. (Color online) Comparison of acoustic transmission data and model outputs in the BIWF area. The 3D and 2D models have small but notable differences in the later arrivals, and they both are comparable to the data. This indicates that the given propagation track has less 3D effects, as shown in Fig. 3.

summary, the propagation model performance is validated from the comparison of its output to a set of measured transmission data, and it is sufficient for making confident predictions to investigate the underwater noise propagation in the BIWF area.

### 4. Analysis of underwater sound propagation

Temporal and spatial variability of sound propagation conditions at BIWF can be analyzed using the integrated acoustic and oceanographic model. Figures 3(a) and 3(b) show 3D propagation of 200 Hz sound, one of the main pile-driving noise frequencies observed in the monitoring data, for two different seasonal (summer and winter) conditions. In each panel, two subplots are shown. The left subplot in each panel shows the water column sound speed at the model source location. The contour plots show the transmission loss (TL) predictions from the sound propagation model. Using the average TL in the two simulations 70 dB as a reference, the propagation distance to the reference TL in winter is ∼10 km farther compared to the distance in summer. At a given distant location, marked by "×" in the TL contours, for example, the TL can differ up to 12 dB at 200 Hz. This enhanced propagation condition in winter when the water column is well-mixed follows the analysis of bottom reflection loss presented in Sec. 2 and is confirmed by the 3D propagation model.

Figures 3(c) and 3(d) are model outputs from neglecting the acoustic coupling in azimuth with an assumption of sound propagation confined in the vertical plane at each radial. This is the $N \times 2D$ type model to create a 3D representation. Comparing the two sets of model outputs we can see that many of the fine scale features predicted by the 3D model and attributed to the horizontal sound focusing and defocusing caused by sea floor irregularity do not appear in the $N \times 2D$ model. This has the

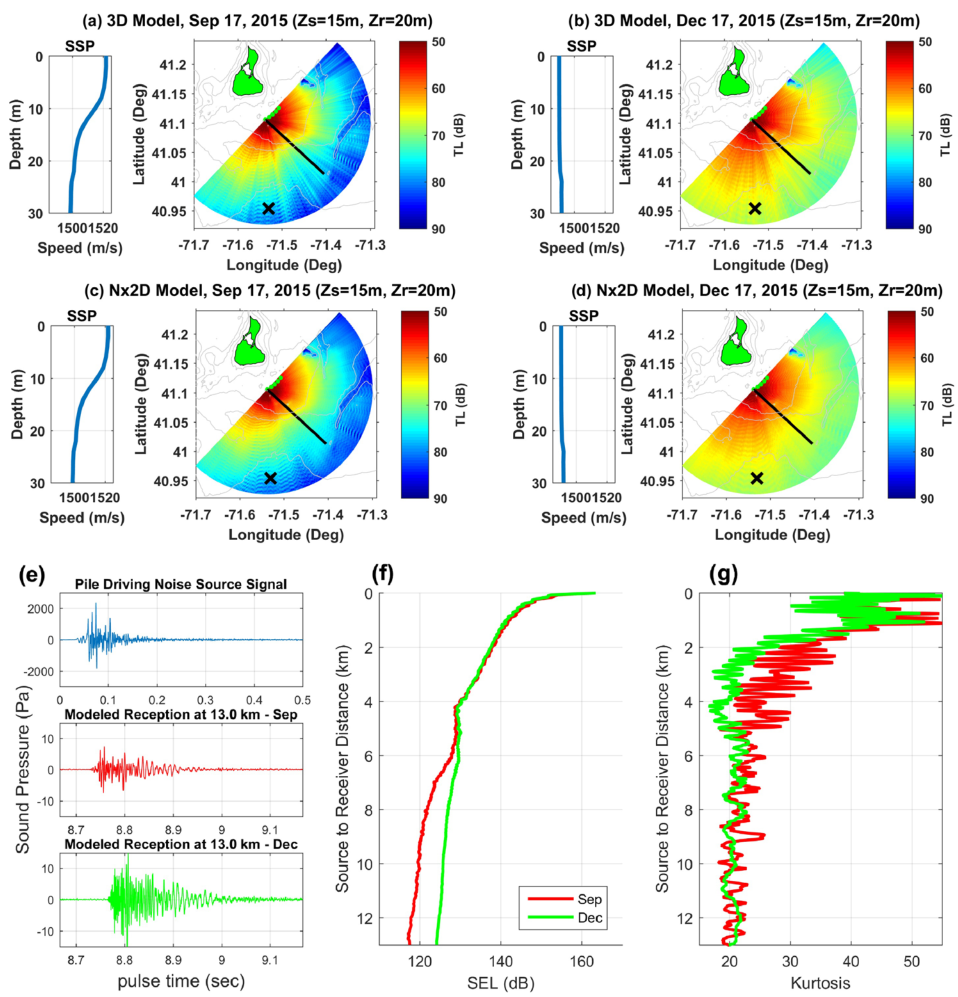


Fig. 3. (Color online) (a) and (b) Seasonal variability of underwater sound propagation of the BIWF area showing TL predictions for 200 Hz sound in September 2015 (summer) and December 2015 (winter). The source depth (Zs) in the model was 15 m, and the receiver depth (Zr) was 20 m. (c) and (d) $N \times 2D$ propagation models. (e)–(g) Pile driving signals simulated using the propagation model in September [middle panel in (e)] and December [lower panel in (e)]. The SELs along the propagation path are shown in (f), while the variations of kurtosis are shown in (g).

potential of creating prediction differences in sound reception levels up to a couple of dB along propagation paths which have significant 3D effects. This model comparison also shows that the propagation track where the transmission validation data were taken (the solid line in the figure) has less 3D effects, as seen in Fig. 2.

The seasonal variability of pile driving signals was analyzed. The modeled propagation path was the validation data track. A line source model for sound radiation from pile driving of the turbine jacket foundation installation was employed. A tetrahedral hydrophone array data was used to provide the pile driving noise source signal. This array was placed just above the sea floor and 500 m from construction sites for Wind Turbine Generators 3 and 4 on a line generally perpendicular to the BIWF turbine array aperture [the red curve in Fig. 1(a)]. The tetrahedral hydrophone array consisted of 4 HTI-94-SSQ hydrophones in a tetrahedral configuration with a 0.5 m spacing and a 9765.625 Hz sampling rate. The hydrophones were calibrated by the manufacturer and all four had sensitivities of $-203.7$ dB re 1 V/$\mu$Pa $\pm$ 0.2 dB. The frequency range in the pile driving sound propagation model was from 17 Hz to 2.5 kHz, which contained 99% of the recorded pile driving sound energy at the tetrahedral array. The pile driving sound at the middle of the water column (20 m) along the propagation track over 15 km was computed. As shown in Figs. 3(e)–3(g), the SELs of pile driving sound at ranges greater than 6 km would be approximately 8 dB less in September when there was a thermocline causing a downward refracting propagation condition and a higher TL as described in the previous simulation study.

Although the September thermocline can yield lower sound levels at longer ranges, the kurtosis of the propagating signals in September are predicted to decay slower at shorter ranges, about 2 to 6 km from the pile as shown in Fig. 3(g). Hence, there are two competing propagation factors in the summer: the sound level decays faster compared to other seasons, but the kurtosis decays slower. Since kurtosis measures infrequent but sudden and peaky intense levels, higher levels of kurtosis indicate possible harmful pressure fluctuations on marine mammals. It is important for marine mammal mitigation planning to consider potential competing factors on sound level and kurtosis, and to reach a balance between them.

## 5. Conclusion

A 3D underwater sound propagation model is established using an accurate wave equation numerical solver[5] with realistic bathymetric and oceanographic inputs from the U.S. CRM high-resolution bathymetry database,[6] the ROMS ESPreSSO regional data-assimilated ocean model,[7] and the NGDC Deck41 seafloor surficial sediment database.[8] The model shows underwater sound propagation at the BIWF has strong seasonal variability, as well as spatial variability down to a kilometer scale.

Although a pile driving sound propagation model is also established, the sound generation mechanism still needs refinement. Also, future model improvement to incorporate surface wind waves and sub-bottom sediment layer structure is required to advance the present model predictions. The ultimate goal is to establish an underwater soundscape modeling, predicting, and planning software system for noise impact management at future wind farm sites. This can be done by also integrating shipping, industrial activities, biological, and non-biological natural processes to assimilate all soundscape components. The applications include predicting the anthropogenic noise impacts on marine mammal habitats and informing management decisions on regulating human activities to manage soundscape ecological changes in the area of offshore marine resource and energy developments.

## Acknowledgments

The authors would like to acknowledge Captain Ken Houlter and First Mate Ian Hanley of the WHOI R/V Tioga. The authors would also like to acknowledge Dr. Steven Crocker from the Naval Undersea Warfare Center in Newport, Rhode Island for the design of the tetrahedral hydrophone array. Study concept, oversight, and funding under the Real-time Opportunity for Development Environmental Operations (RODEO) were provided by the U.S. Department of the Interior, Bureau of Ocean Energy Management, Environmental Studies Program, Washington, DC under Contract No. M16PD00025. The Program Manager at BOEM is Dr. Mary Boatman. The prime contractor for this work is HDR, Inc. (Program Manager Anwar Khan).

## References and links

[1]Deepwater Wind, "America's First Offshore Wind Farm Powers Up," available at http://dwwind.com/press/americas-first-offshore-wind-farm-powers/ (Last viewed February 16, 2019).

[2]HDR "Underwater Acoustic Monitoring Data Analyses for the Block Island Wind Farm, Rhode Island," Final Report to the U.S. Department of the Interior, Bureau of Ocean Energy Management, Office of Renewable Energy Programs, OCS Study BOEM 2018 (2019).
[3]B. L. Southall, A. E. Bowles, W. T. Ellison, J. J. Finneran, R. L. Gentry, C. R. Greene, Jr., D. Kastak, D. R. Ketten, J. H. Miller, P. E. Nachtigall, W. J. Richardson, J. A. Thomas, and P. L. Tyack, "Marine mammal noise exposure criteria: Initial scientific recommendations," Aquat. Mamm. **33**(4), 411–521 (2007).
[4]D. H. Shonting and G. S. Cook, "On the seasonal distribution of temperature and salinity in Rhode Island sound," Limnology Oceanograph. **15**(1), 100–112 (1970).
[5]Y.-T. Lin, T. F. Duda, and A. E. Newhall, "Three-dimensional sound propagation models using the parabolic-equation approximation and the split-step Fourier method," J. Comp. Acoust. **21**, 1250018 (2013).
[6]National Geophysical Data Center, "U.S. Coastal Relief Model—Northeast Atlantic," National Geophysical Data Center, NOAA (1999).
[7]Rutgers Ocean Modeling Group, "ESPRESSO ocean modeling from Rutgers ROMS group," available at http://www.myroms.org/espresso/ (Last viewed February 16, 2019).
[8]National Geophysical Data Center (NGDC), and National Oceanic Data Center (NODC), 200310, Seafloor Surficial Sediment Descriptions (Deck41) NGDC Data Set G02094.